Transition Location Effect on Oblique Shock-Wave/Boundary-Layer Interaction at M=1.5

A. Sansica, N. D. Sandham, and Z. Hu

Abstract The effect of transition location on the interaction between an oblique shock-wave and a boundary-layer at $M = 1.5$ on a flat plate is investigated via direct numerical simulations. It is shown that the shock trips transition at the impingement location and the effect of the impingement location on the separation is studied for laminar, transitional and turbulent interactions. Qualitative agreement is obtained with the experiments, as part of the European FP7-2012 TFAST project.

1 Introduction

In high speed flows over wings and in gas turbines, shock-wave/boundary-layer interaction (SWBLI) can occur and cause separation, transition to turbulence and unsteadiness near the interaction region. SWBLI has been an important topic for the aeronautical scientific community over the past 60 years with most of the work carried out for turbulent interactions. Laminar and transitional interactions are also of interest because they can occur in wind tunnel testing, on turbine and compressor blades and on wings and intakes. The present work considers the effect of transition location on the interaction between an oblique shock-wave and a boundary-layer at $M = 1.5$ on a flat plate. Experiments conducted at the Institute of Theoretical and Applied Mechanics (ITAM) in Novosibirsk, Russia for laminar, transitional and turbulent interactions are used for comparisons.

A. Sansica e-mail: A.Sansica@soton.ac.uk · N. D. Sandham · Z. Hu
Aerodynamics and Flight Mechanics Research Group, Faculty of Engineering and the Environment, University of Southampton, Southampton SO17 1BJ, United Kingdom

2 Numerical Method

As part of the European Union (EU) FP7-2012 project TFAST (`http://www.tfast.eu`), different interaction types have been investigated numerically with a compressible in-house high-order fully-parallelised finite difference code. More details and validation of the code can be found in Sansica *et al.* [1]. The numerical setup is based on the experiments carried out by ITAM and three different types of interaction are studied. By moving the shock wave in the streamwise direction it is possible to obtain laminar, transitional and turbulent interactions, depending on the state of the zero-pressure gradient (ZPG) boundary-layer just upstream of the impingement location. The free-stream Mach number is $M = 1.5$, free-stream temperature $T_\infty^* = 197.93\,K$ and Sutherland's law is used to describe the variation of viscosity μ with the temperature (Sutherland's constant is taken as $T_S^* = 110.4\,K$). For all simulations, the inflow boundary is placed at $x_0 = 0.0518\,m$ downstream of the flat plate leading edge where the displacement thickness is $\delta_{1,0}^* = 1.84 \times 10^{-4}\,m$ and giving a Reynolds number based on the displacement thickness at the inlet of $Re_{\delta_{1,0}^*} = 1971.07$. The angle of the shock generator plate is fixed to $\theta = 4^\circ$ for all the SWBLI cases. Depending on the interaction type, the streamwise domain length, L_x, is increased in order to let the boundary-layer become either transitional or turbulent before the interaction. Thus, $L_x/\delta_{1,0}^* = 175, 250$ and 350 for the laminar, transitional and turbulent interactions, respectively. For all cases, the domain height is fixed to be $L_y/\delta_{1,0}^* = 90$ in order to avoid any possible reflection of the wave system from the top boundary impinging onto the boundary-layer. The span width is to $L_z/\delta_{1,0}^* = 2\pi/\beta = 31$, where β is the spanwise wavenumber of the most unstable mode predicted by local linear stability theory (LST) at the inflow. The grid is uniform in the spanwise direction, z, and stretched in the wall-normal direction, y, clustering about 30% of the grid points within the boundary-layer at the inlet. The grid distribution in the streamwise direction is refined at either the shock impingement or the transition location (whichever comes first). The number of grid points is $(n_x, n_y, n_z) = (1824, 288, 462)$ for the laminar interaction, $(2400, 288, 462)$ for the transitional one and $(2976, 288, 462)$ for the turbulent case. In wall units, the grid resolution in the transitional/turbulent region is $\Delta x^+ = 4.8$, $\Delta z^+ = 4.8$ and $\Delta y^+_{wall} = 0.96$. For the ZPG boundary-layer study, the same domain size and grid resolution as for the turbulent interaction are used. The boundary conditions applied to the computational domain are no-slip and fixed temperature (with temperature equal to the laminar adiabatic wall temperature) at the wall. To minimise the reflection of waves into the domain, an integral characteristic method is applied to the top boundary and a standard characteristic boundary condition at the outflow. A similarity solution profile is applied at the inlet and the boundary-layer is forced with a time-dependent boundary condition. A "broadband modal" forcing technique is used and consists in the forcing of 42 eigenmodes calculated with local LST at the inlet for different combinations of frequency and spanwise wavenumber. Random phases are added to each mode in order to break any symmetries.

3 Results

Forcing is applied to a ZPG boundary-layer with an amplitude of $A_o = 0.05$ (corresponding to a turbulence intensity at the inflow $\rho_{rms} = 0.25\%$). The time and span averaged skin friction distribution (a) and instantaneous streamwise velocity at the centre plane (b) reported in Fig. 1 show that transition starts at $Re_x = 7 \times 10^5$ and the turbulent state is reached at $Re_x = 11 \times 10^5$. An overshoot of the skin friction with respect to empirical distribution from Young (1989) [3] can be seen for $Re_x \geq 1.02 \times 10^6$ due to the high intensity structures formed during the breakdown to turbulence. The main transition scenario is a bypass breakdown where intermittent turbulent spots are generated. Fig. 2 shows the contours of vertical vorticity in the vicinity of the wall for two different time instances: $t = 7,900$ (a) and $t = 8,350$ (b). The formation of a turbulent spot is visible in Fig. 2-b between $Re_x = 9 \times 10^5$ and $Re_x = 10.5 \times 10^5$. Three different impingement locations are selected and de-

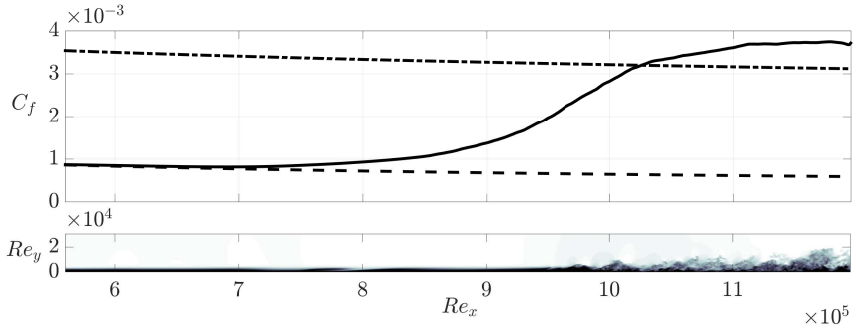

Fig. 1 ZPG boundary-layer case: (a) Time and span averaged skin friction distribution (solid line) along with laminar (dashed line) and turbulent (dash-dotted line) boundary-layer distributions by Eckert (1955) [2] and Young (1989) [3], respectively; (b) contours of instantaneous streamwise velocity.

fine laminar, transitional and turbulent interactions at an impingement Reynolds number $Re_{x_{imp^*}}(\times 10^5) = 7.6, 8.9$ and 10.2, respectively. Span and time averaged skin friction distributions are reported in Fig. 3 for both the ZPG boundary-layer and the interaction cases. A first main observation is that when a laminar interaction occurs the boundary-layer separates, while it remains attached for the turbulent interaction. For the transitional case, a marginal separation occurs. As part of the TFAST project, Giepman *et al.* [4] reported a similar situation for different SWBLIs at $M = 1.7$. While the separated region is large for the laminar interaction, for the transitional case the zone of reversed flow is significantly reduced and no mean-flow separation is present for the turbulent interaction. Another important point, in qualitative agreement with the experiments, is that a turbulent boundary-layer is detected immediately downstream of the impingement location for the laminar interaction and that transition is accelerated for the transitional and turbulent cases. The shock is very strong and the boundary-layer becomes turbulent at the shock

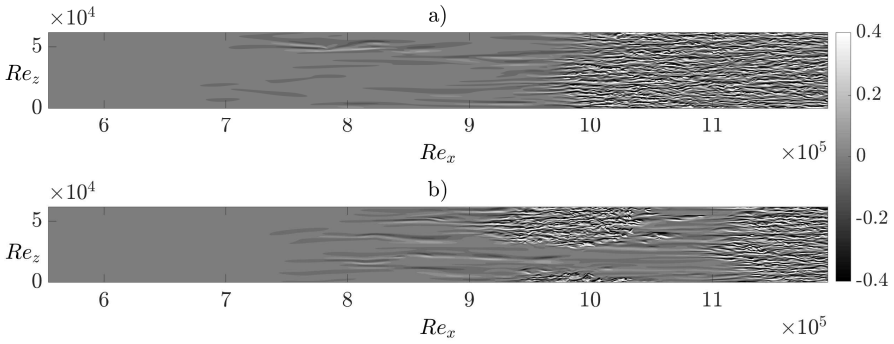

Fig. 2 ZPG boundary-layer case: Contours of vertical vorticity at time levels $t = 7,900$ (a) and $t = 8,350$ (b).

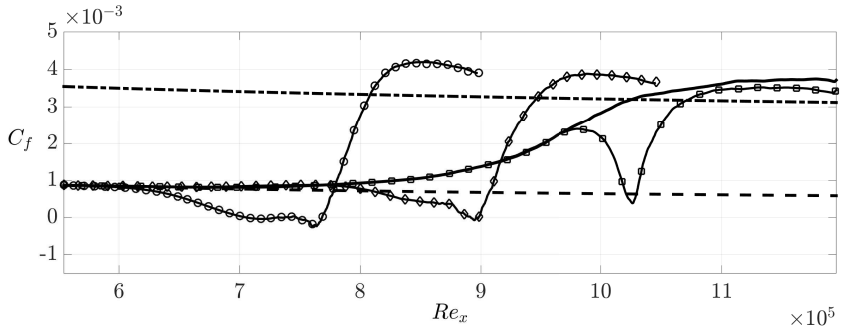

Fig. 3 Time and span averaged skin friction distribution for the laminar (solid line with circles), transitional (solid line with diamonds) and turbulent (solid line with squares) interactions. The ZPG boundary-layer (solid line) is also plotted along with laminar (dashed line) and turbulent (dash-dotted line) boundary-layer distributions by Eckert (1955) [2] and Young (1989) [3], respectively.

impingement location. A useful way to determine the state of the boundary-layer is to calculate an intermittency function, Γ, calculated as the fraction of time during which the first and second time derivatives of the skin friction time series are larger than a prescribed threshold, indicating that the boundary-layer is locally turbulent. The span-averaged intermittency distributions for the ZPG boundary-layer case and the interaction cases are reported in Fig. 4-a. The intermittency distributions show a sharp increase towards unity downstream of the impingement location due to the turbulent character of the boundary-layer. Upstream of the impingement, the effect of the shock-wave differs significantly, depending on the type of interaction. For the laminar interaction, the boundary-layer quickly switches from being laminar to turbulent when passing across the shock and this causes a very localised change of the intermittency. The transitional interaction affects the boundary-layer for a longer upstream extent and the increase of intermittency is more gradual. Although the boundary-layer stays attached, the presence of the interaction changes the instability of the boundary-layer and the Γ distribution deviates from the ZPG

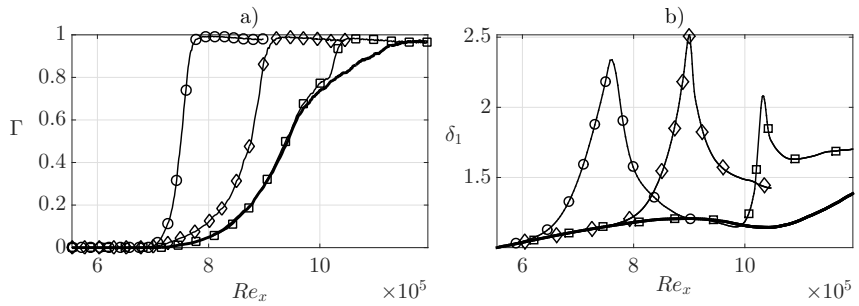

Fig. 4 Span averaged intermittency (a) and displacement thickness (b) distributions for ZPG boundary-layer case (solid line) and the laminar (solid line with circles), transitional (solid line with diamonds) and turbulent (solid line with squares) interactions.

distribution. This also happens for the turbulent case but with less significant consequences since the size of the interaction is much smaller. The upstream response of the boundary-layer to the turbulent interaction is negligible and the major effects are only visible downstream of the impingement, for example on the thickening of the boundary-layer. The time and span averaged displacement thickness distributions, δ_1, reported in Fig. 4-b show that the boundary-layer thickening after the interaction increases with $Re_{x^*_{imp}}$, especially for the transitional and turbulent interactions whose thickening is significantly larger than the ZPG case. Another important difference between the three interactions is the unsteady character of the shock at the impingement. Oil flow visualisations around the shock impingement location provided by ITAM can be used for a qualitative comparison. Fig. 5 compares the experimental oil flow visualisations with the DNS statistical skin friction distributions for each interaction. For better clarity, the DNS visualisations are scaled up by a factor of about 2 with respect to the original size, which is indicated in the black rectangle in the oil flow picture (the spanwise location is purely indicative). For the laminar interaction, the paint in the oil flow visualisation is spread significantly upstream of the shock impingement location due to the existence of the separation bubble. For the transitional interaction, the shock location is clearly indicated by the vertical black region. However, the presence of turbulent spots moving through the shock smear the paint and leave localised horizontal traces of paint across the vertical black line. In the same way, the DNS skin friction shows elongated structures upstream of the impingement. For the turbulent case, both experiments and DNS show a narrow vertical black line resulting from a relatively steady interaction.

4 Conclusions

Direct numerical simulations are performed to investigate laminar, transitional and turbulent interactions of a boundary-layer with an imposed oblique shock. Displace-

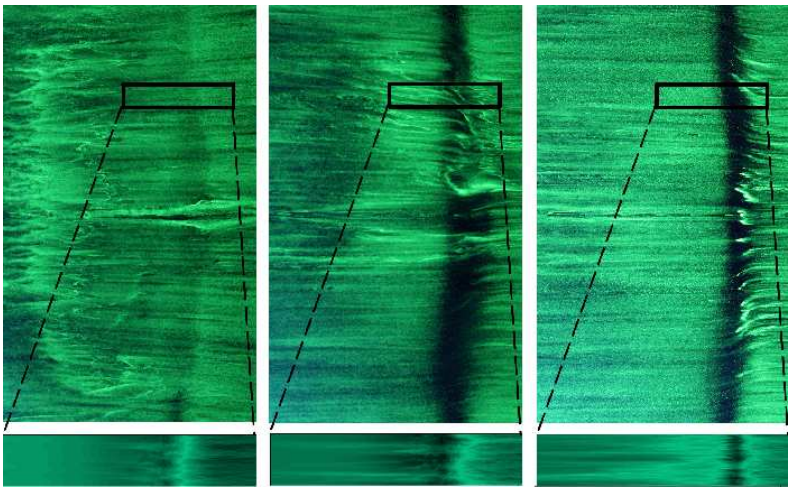

Fig. 5 Oil flow visualisations by ITAM (top plots) for laminar (left), transitional (middle) and turbulent (right) interactions. Comparisons with statistical DNS skin friction distributions (bottom plots). [With permission of A. A. Sidorenko and P. A. Polivanov (ITAM, Novosibirsk, Russia)]

ment thickness and intermittency distributions are used to distinguish the different types of interaction. In agreement with the experiments, the boundary-layer is separated for laminar interactions while it remains attached for transitional and turbulent ones. The oblique shock trips the boundary-layer at the impingement location for the laminar case, while it accelerates transition for the transitional and turbulent interactions. Differently to laminar and transitional cases, the effects of the turbulent interaction upstream of the impingement are minor. Qualitative agreement is achieved between the numerical simulations and experimental data.

Acknowledgements This work is supported through the European Union (EU) FP7 project TFAST. Computer time is provided by Engineering and Physical Sciences Research Council (EPSRC, UK), under Grant No. EP/L000261/1. Experimental data are provided by A. A. Sidorenko and P. A. Polivanov (ITAM, Novosibirsk, Russia).

References

1. Sansica, A., Sandham, N. D., and Hu, Z.: Forced response of a laminar shock-induced separation bubble. Physics of Fluids, **26**, 093601 (2014)
2. Eckert, E. R. G.: Engineering Relations for Friction and Heat Transfer to Surfaces in High Velocity Flow. J. of Aeronautical Sciences, **2**, 585-587 (1955)
3. Young, A. D.: Boundary Layers. AIAA Educational Ser., Blackwell Science (1989)
4. Giepman, R. H. M., Schrijer, F. F. J., and van Oudheusden, B. W.: High resolution PIV measurements of a transitional shock wave boundary layer interaction. Experiments in Fluids, **56**, 120 (2015)